Hopf bifurcation in REM congestion control under gamma-distributed feedback delays

Hopf bifurcation in REM congestion control under gamma-distributed feedback delays

Carlo Bianca[1,⋆], Luca Guerrini[2], Stefania Ragni[3]

[1] EFREI Research Lab, Université Paris-Panthéon-Assas, 30/32 Avenue de la République, 94800 Villejuif, France
[2] Department of Management, Polytechnic University of Marche, Ancona, Italy
[3] Department of Economics and Management, University of Ferrara, Ferrara, Italy.

⋆ *Corresponding Author*. carlo.bianca@efrei.fr

Abstract. This paper is devoted to the stability analysis and Hopf bifurcation of a REM-based congestion control algorithm with gamma-distributed feedback delays, a more realistic alternative to conventional constant-delay models. By employing the linear chain trick, which allows to transform To capture delay variability due to queuing, routing, and protocol overhead, we model the system using gamma-distributed kernels and convert the resulting integro-differential equations into finite-dimensional ODEs, we show explicit delay thresholds for the onset of bifurcations under two memory regimes, called weak and strong regimes. In the weak memory case, a single critical delay governs stability, whereas strong memory induces stability only within a bounded delay interval. Numerical investigations confirm that distributed-delay models exhibit smoother transitions to instability and generate oscillations consistent with supercritical Hopf bifurcations. Compared to traditional discrete-delay REM models, our formulation offers superior robustness and smoother bifurcation dynamics. These findings provide actionable insights for delay-aware congestion control design in heterogeneous network environments.

1 Introduction

The stability of congestion control protocols in the presence of communication delays is a critical issue in network control theory. A seminal work by [1] investigated the behavior of the Random Exponential Marking (REM) algorithm under constant feedback delays and demonstrated that the system experiences a Hopf bifurcation when the round-trip delay exceeds a critical threshold. The

[2010] **Mathematics Subject Classification** 34K20, 37G15, 90B18
Keywords: Distributed delay; Hopf bifurcation; Congestion control; Gamma kernels.

model, which consists of a system of delay differential equations, revealed that increased delay leads to a destabilization of the equilibrium and the emergence of periodic oscillations in both queue lengths and congestion pricing. The center manifold theorem and normal form theory [2] have been employed to characterize the stability and direction of the bifurcating periodic solutions. Yang and Tian's work extends the Internet congestion control framework developed by Low and Lapsley [3], which modeled TCP/AQM dynamics as a primal-dual optimization process. REM was designed by Athuraliya et al. [4] to decouple performance and congestion measures. Yin and Low [5, 6] confirmed REM's convergence under zero or uniform delay assumptions, while Paganini [7] proved its global asymptotic stability. However, these results did not account for feedback delay, which is ever-present in real networks. Related models include earlier work by Li et al. [8], who analyzed Hopf bifurcation in a first-order congestion control model using control gain as the bifurcation parameter, unlike [1], which uses delay as the bifurcation parameter. Tian and Yang [9] had also shown that diverse delay structures can induce nontrivial dynamic effects in TCP/AQM systems.

Despite these advances, the assumption of fixed or discrete delays remains a simplification. In practical networks, round-trip times are influenced by routing changes, queuing variability, protocol processing, and retransmission events. To better model this uncertainty, distributed delay models have been proposed. [10] presented one of the first analyses of bifurcation behavior in a REM-like system with distributed delay kernels, showing that such systems can have broader and more resilient stability properties. More recently, [11] studied dual-delay congestion control mechanisms that reflect the bidirectional delay characteristics seen in real-time communications. The practical relevance of distributed delay models is further supported by engineering applications. [12] developed HetFlow, a delay-aware data center congestion controller that improves performance under delay variability. [13] designed a cross-datacenter control protocol that uses real-time feedback to adapt to fluctuating round-trip times. Likewise, [14] proposed a delay-resilient resource allocation strategy for vehicular networks. Mathematically, the use of distributed delays leads to integro-differential equations that are challenging to analyze directly. A powerful technique to handle such systems is the linear chain trick, which transforms the convolutional memory terms into auxiliary differential equations. This method has been employed successfully in a range of domains, including fractional and fuzzy systems [15, 16, 17, 18, 19].

This paper extends the classical REM framework proposed by [1] by incorporating gamma-distributed feedback delays. We analyze two delay regimes, weak memory and strong memory, and derive the related bifurcation conditions. The results show that distributed-delay systems exhibit smoother transitions to instability and can maintain equilibrium over a wider range of delay parameters. These insights contribute to the design of more robust congestion control protocols in heterogeneous and delay-sensitive network environments.

The rest of the paper is organized as follows. In Section 2, we introduce the mathematical model of REM with gamma-distributed delays and derive the equivalent system of ODEs using the linear chain trick. Section 3 analyzes the stability and Hopf bifurcation behavior in the weak memory case ($m = 1$), while Section 4 extends the analysis to the strong memory regime ($m = 2$). Section 5 presents numerical simulations that validate the theoretical results and illustrate the dynamic implications of distributed delay structures. Finally, Section 6 summarizes the main findings and outlines possible directions for future research.

2 The distributed delays model

Following Yang and Tian framework, the REM model consists of the following DDEs:

$$\begin{cases} \dot{b}(t) = F(p(t-D)) - c, \\ \dot{p}(t) = \gamma[b(t) - b_0 + F(p(t-D)) - c], \end{cases} \tag{2.1}$$

where $b(t)$ is the buffer size (queue length) at time t, $p(t)$ is the congestion price (marking rate), $F(p)$ is the rate adjustment function, D is the round-trip communication delay, γ is the control gain, c is the link service capacity, b_0 is the target buffer length. In this formulation, the source adjusts its sending rate based on outdated congestion price information due to the constant delay D. To capture the more realistic scenario where feedback delays are distributed over time, we replace the discrete delay in (2.1) with a convolution integral over the past values of $p(t)$. This leads to the following distributed delay system:

$$\begin{cases} \dot{b}(t) = F\left(\int_0^\infty p(t-u)g(u)\,du\right) - c, \\ \dot{p}(t) = \gamma\left[b(t) - b_0 + F\left(\int_0^\infty p(t-u)g(u)\,du\right) - c\right], \end{cases} \tag{2.2}$$

where $g(u)$ is the delayed kernel defined by the following gamma distribution:

$$g(u) = \frac{m^m}{T^m(m-1)!}u^{m-1}e^{-\frac{m}{T}u}, \quad u \geq 0,$$

with shape parameter $m \in \mathbb{N}$, scale parameter (mean delay) $T > 0$, and normalization condition

$$\int_0^\infty g(u)\,du = 1.$$

This representation introduces memory effects into the model, as the present congestion price update depends on a weighted history of past prices. The distributed delay model (2.2) involves an integral term that is analytically challenging to handle. To facilitate analysis, we apply the linear chain trick, which exploits the recursive structure of the gamma kernel to reformulate the integral as a system of ODEs. The key idea is to represent the convolution as the solution to an auxiliary dynamical system involving intermediate variables. The resulting ODE systems retain the essential memory characteristics of the distributed delay model while enabling classical tools such as linearization, eigenvalue analysis, and bifurcation theory. In the following sections, we explicitly derive the ODE systems for $m = 1$ (weak delay) and $m = 2$ (strong delay), and analyze the conditions under which the REM system undergoes delay-induced instability and periodic oscillations.

3 Stability and Hopf bifurcation: Weak delay regime

For $m = 1$, the gamma delay kernel reads:

$$g(u) = \frac{1}{T}e^{-u/T}, \quad u \geq 0,$$

representing a memory less exponential delay. Using the linear chain trick, we introduce the following function:

$$u(t) = \int_0^\infty p(t-r) \cdot \frac{1}{T} e^{-r/T}\, dr,$$

and transform the distributed delay model (2.2) into the following system of ordinary differential equations:

$$\begin{cases} \dot{b} = F(u) - c, \\ \dot{u} = \dfrac{1}{T}(p-u), \\ \dot{p} = \gamma[\alpha(b-b_0) + F(u) - c]. \end{cases} \tag{3.1}$$

The equilibrium point of this system is denoted by (b^*, u^*, p^*), where $b^* = b_0$, $F(u^*) = c$, and $p^* = u^*$. Linearizing system (3.1) around the equilibrium yields the following characteristic equation:

$$\begin{vmatrix} -\lambda & F'(u^*) & 0 \\ 0 & -\dfrac{1}{T} - \lambda & \dfrac{1}{T} \\ \alpha\gamma & \gamma F'(u^*) & -\lambda \end{vmatrix} = 0,$$

which leads to the cubic polynomial

$$\lambda^3 + a_1(T)\lambda^2 + a_2(T)\lambda + a_3(T) = 0, \tag{3.2}$$

where

$$a_1(T) = \frac{1}{T} > 0, \quad a_2(T) = -\frac{\gamma F'(u^*)}{T} > 0, \quad a_3(T) = -\frac{\alpha\gamma F'(u^*)}{T} > 0.$$

According to the Routh-Hurwitz criterion, the equilibrium is locally asymptotically stable if and only if

$$a_1(T)a_2(T) - a_3(T) > 0,$$

which simplifies to

$$T < \frac{1}{\alpha}.$$

Thus, the critical delay threshold is

$$T^* = \frac{1}{\alpha},$$

which separates the stable regime ($T < T^*$) from the unstable regime ($T > T^*$). At $T = T^*$, the system undergoes a Hopf bifurcation. At the bifurcation threshold $T = T^*$, the characteristic equation (3.2) rewrites as

$$[\lambda + a_1(T^*)][\lambda^2 + a_2(T^*)] = 0.$$

Hence, the eigenvalues read:

$$\lambda_{1,2} = \pm i\sqrt{a_2(T^*)} = \pm i\omega^*, \quad \lambda_3 = -a_1(T^*) = -\frac{1}{T^*} < 0.$$

To confirm the existence of a Hopf bifurcation, we differentiate (3.2) with respect to T, and get

$$\left[3\lambda^2+2a_1(T)\lambda+a_2(T)\right]\frac{d\lambda}{dT}=-\left[a_1'(T)\lambda^2+a_2'(T)\lambda+a_3'(T)\right], \tag{3.3}$$

where

$$a_1'(T)=-\frac{1}{T^2}>0,\quad a_2'(T)=\frac{\gamma F'(u^*)}{T^2}>0,\quad a_3'(T)=\frac{\alpha\gamma F'(u^*)}{T^2}>0.$$

Substituting $\lambda=i\omega^*$ into (3.3), we compute the transversality condition

$$\mathrm{Re}\left(\frac{d\lambda}{dT}\bigg|_{\lambda=i\omega^*}\right)=-\frac{\alpha^2\gamma F'(u^*)}{2[-\gamma F'(u^*)+\alpha]}>0,$$

which indicates that the pair of complex conjugate eigenvalues crosses the imaginary axis with nonzero speed, confirming a Hopf bifurcation occurs at $T=T^*$. We summarize the stability and bifurcation behavior for $m=1$ in the following theorem.

Theorem 3.1. The equilibrium point (b^*,u^*,p^*) of system (3.1) is locally asymptotically stable for all $T<T^*$ and unstable for $T>T^*$. Moreover, the system undergoes a Hopf bifurcation at $T=T^*$.

4 Stability and Hopf bifurcation: Strong delay regime

We now analyze the system behavior in the case of a strong delay kernel, corresponding to the gamma distribution with shape parameter $m=2$. This choice models stronger memory effects, where delay values are more concentrated around their mean. As before, we employ the linear chain trick to convert the original distributed delay system into an equivalent finite-dimensional system of ordinary differential equations. Defining the new variables

$$v(t)=\int_{-\infty}^{t}p(r)\left(\frac{2}{T}\right)^2(t-r)e^{-\frac{2}{T}(t-r)}dr,\quad w(t)=\int_{-\infty}^{t}p(r)\left(\frac{2}{T}\right)e^{-\frac{2}{T}(t-r)}dr,$$

system (2.2) writes:

$$\begin{cases}\dot b=F(v)-c,\\ \dot v=\dfrac{2}{T}(w-v),\\ \dot w=\dfrac{2}{T}(p-w),\\ \dot p=\gamma[\alpha(b-b_0)+F(v)-c].\end{cases} \tag{4.1}$$

We consider the equilibrium point (b^*,v^*,w^*,p^*), where $b^*=b_0$, $F(v^*)=c$, and $w^*=p^*=v^*$. The characteristic equation of the linearized system around the equilibrium point is given by

$$\begin{vmatrix}-\lambda & F'(v^*) & 0 & 0\\ 0 & -\frac{2}{T}-\lambda & \frac{2}{T} & 0\\ 0 & 0 & -\frac{2}{T}-\lambda & \frac{2}{T}\\ \alpha\gamma & \gamma F'(v^*) & 0 & -\lambda\end{vmatrix}=0,$$

which yields the fourth-degree algebraic equation:

$$\lambda^4 + a_1(T)\lambda^3 + a_2(T)\lambda^2 + a_3(T)\lambda + a_4(T) = 0, \tag{4.2}$$

where the coefficients are defined by

$$a_1(T) = \frac{4}{T}, \quad a_2(T) = \frac{4}{T^2}, \quad a_3(T) = -\frac{4\gamma F'(v^*)}{T}, \quad a_4(T) = -\frac{4\alpha\gamma F'(v^*)}{T^2}.$$

According to the Routh–Hurwitz criterion, the equilibrium point is locally asymptotically stable if and only if

$$\Psi(T) = a_1(T)a_2(T)a_3(T) - a_3^2(T) - a_1^2(T)a_4(T) > 0. \tag{4.3}$$

The inequality (4.3) holds if and only if

$$-\gamma F'(v^*)T^4 - 4T^2 + 4\alpha < 0. \tag{4.4}$$

The discriminant of this inequality is

$$\Delta = 16\left[1 + \alpha\gamma F'(v^*)\right].$$

Three scenarios can occur

1) If $\Delta < 0$, the inequality (4.4) is never satisfied, and $\Psi(T) > 0$ does not hold for any T.
2) If $\Delta = 0$, the inequality (4.4) reduces to a squared term and again fails to satisfy $\Psi(T) > 0$.
3) If $\Delta > 0$, the inequality (4.4) is satisfied for

$$T_1^* = \sqrt{-\frac{2}{\gamma F'(v^*)}\left(1 - \sqrt{1 + \alpha F'(v^*)}\right)}, \quad T_2^* = \sqrt{-\frac{2}{\gamma F'(v^*)}\left(1 + \sqrt{1 + \alpha F'(v^*)}\right)}. \tag{4.5}$$

Therefore, $\Psi(T) > 0$ if and only if $T_1^* < T < T_2^*$ and $1 + \alpha\gamma F'(v^*) > 0$. The values $T = T_1^*$ and $T = T_2^*$ define the bifurcation boundaries between stable and unstable regimes. At $T = T^*$, the characteristic equation (4.2) factors as follows:

$$\left[a_1(T^*)\lambda^2 + a_3(T^*)\right]\left[a_1(T^*)\lambda^2 + a_1^2(T^*)\lambda + a_1(T^*)a_2(T^*) - a_3(T^*)\right] = 0.$$

This factorization yields:

$$\lambda_{1,2} = \pm i\sqrt{-\frac{\gamma F'(v^*)}{a_1(T^*)}}, \quad \lambda_{3,4} = -\frac{2}{T} \pm \sqrt{-\gamma F'(v^*)}.$$

To confirm the occurrence of Hopf bifurcation, we consider the characteristic roots as continuous functions of T and differentiate equation (4.2) with respect to T:

$$\left[4\lambda^3 + 3a_1(T)\lambda^2 + 2a_2(T)\lambda + a_3(T)\right]\frac{d\lambda}{dT} = -\left[a_1'(T)\lambda^3 + a_2'(T)\lambda^2 + a_3'(T)\lambda + a_4'(T)\right], \tag{4.6}$$

with

$$a_1'(T) = -\frac{4}{T^2}, \quad a_2'(T) = -\frac{8}{T^3}, \quad a_3'(T) = \frac{4\gamma F'(v^*)}{T^2}, \quad a_4'(T) = \frac{8\alpha\gamma F'(v^*)}{T^3}.$$

Substituting $\lambda = i\omega^*$ into (4.6), we obtain

$$\mathrm{Re}\left(\left.\frac{d\lambda}{dT}\right|_{\lambda=i\omega^*}\right) = -\frac{a_1(T^*)\Psi'(T^*)}{2\left\{a_1^2(T^*)a_3(T^*)+\omega_*^2\left[a_1(T^*)a_2(T^*)-2a_3(T^*)\right]\right\}}, \tag{4.7}$$

where

$$\Psi'(T^*) = a_1'(T^*)a_2(T^*)a_3(T^*)+a_1(T^*)a_2'(T^*)a_3(T^*)+a_1(T^*)a_2(T^*)a_3'(T^*) \\ -2a_3(T^*)a_3'(T^*)-2a_1(T^*)a_1'(T^*)a_4(T^*)-a_1^2(T^*)a_4'(T^*).$$

After simplification, we obtain

$$\Psi'(T^*) = -\frac{32\gamma F'(v^*)}{T^{*5}}\left(8\alpha-3-\gamma F'(v^*)T^{*2}\right).$$

From (4.5), we derive

$$-\gamma F'(v^*)(T_1^*)^2 = 2\left[1-\sqrt{1+\alpha F'(v^*)}\right], \quad -\gamma F'(v^*)(T_2^*)^2 = 2\left[1+\sqrt{1+\alpha F'(v^*)}\right].$$

Hence

$$\Psi'(T^*) = -\frac{32\gamma F'(v^*)}{T^{*5}}\left[8\alpha-1\pm\sqrt{1+\alpha F'(v^*)}\right],$$

where the "+"corresponds to T_1^*, and the "−"to T_2^*. Thus, (4.7) leads to

$$\mathrm{sign}\left[\mathrm{Re}\left(\left.\frac{d\lambda}{dT}\right|_{\lambda=i\omega^*}\right)\right] = \mathrm{sign}\left[1-8\alpha\mp\sqrt{1+\alpha F'(v^*)}\right]. \tag{4.8}$$

As T increases, a positive sign of (4.8) indicates that an eigenvalue crosses the imaginary axis from left to right, signaling a potential loss of stability. Conversely, a negative sign implies crossing from right to left, indicating a possible stabilization of the system. In conclusion, we obtain the following result.

Theorem 4.1. The equilibrium point (b^*, v^*, w^*, p^*) of system (4.1) is locally asymptotically stable for $T_1^* < T < T_2^*$ and $1+\alpha\gamma F'(v^*) > 0$, and unstable otherwise. A Hopf bifurcation may occur at $T = T_1^*$ or $T = T_2^*$.

5 Numerical Simulations

To validate the analytical results and replicate the benchmark simulations of [1], we simulate the REM congestion control model under the original nonlinear adjustment function

$$F(p) = \frac{m}{p},$$

with $m = 0.1$, which corresponds to a logarithmic utility function $U(x) = \ln(x)$ commonly used in congestion economics. We consider the following fixed parameter values throughout the simulations: the link capacity is set to $c = 1$, the desired buffer size to $b_0 = 10$, the congestion sensitivity (control gain) to $\gamma = 0.05$, and the proportional coefficient on queue deviation to $\alpha = 0.005$. The steady-state values are $p^* = 0.1$ and $b^* = 10$. To investigate the influence of communication delay on system behavior, we examine two cases: i) a subcritical delay $D = 2$, which lies below the Hopf bifurcation

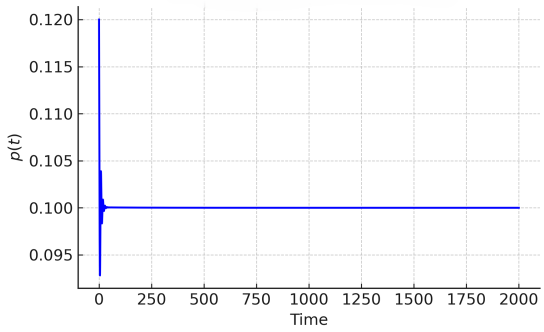

Fig. 1 $p(t)$ vs Time for $D = 2$ (stable regime)

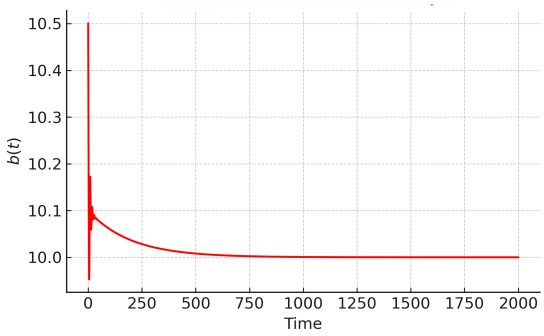

Fig. 2 $b(t)$ vs Time for $D = 2$ (stable regime)

threshold $D_0 \approx 3.1214$, and ii) a supercritical delay $D = 4$, which lies beyond the threshold and induces oscillatory dynamics.

Figures 1 and 2 show the time evolution of the congestion price $p(t)$ and queue length $b(t)$ for $D = 2$. The trajectories converge monotonically to their equilibrium values, confirming the system's local asymptotic stability. Economically, this behavior indicates a well-tuned congestion response where users adjust sending rates in accordance with system feedback, maintaining steady queue occupancy and price levels. As the delay increases to $D = 4$, exceeding the theoretical threshold D_0, the

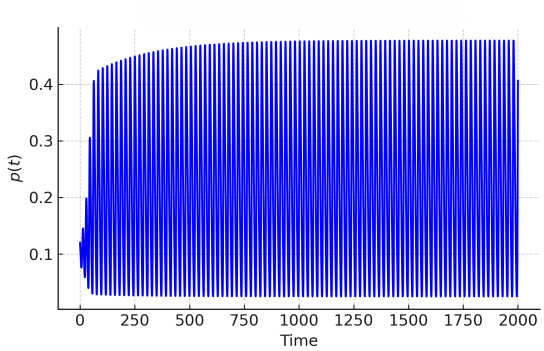

Fig. 3 $p(t)$ vs Time for $D = 4$ (oscillatory regime)

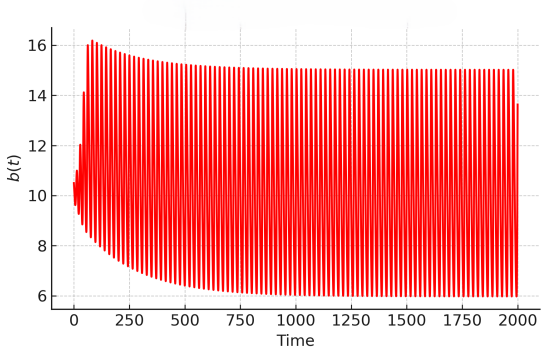

Fig. 4 $b(t)$ vs Time for $D = 4$ (oscillatory regime)

system undergoes a Hopf bifurcation. This is confirmed by the emergence of sustained oscillations in both $p(t)$ and $b(t)$, as shown in Figures 3 and 4. The dynamics are periodic and persistent, indicating the birth of a stable limit cycle. From an economic perspective, these oscillations reflect an endogenous instability in network pricing and congestion control. The system cycles between underutilization and overload, creating fluctuations in buffer occupancy and congestion prices. Such behavior undermines efficiency and can degrade quality-of-service, especially in high-demand scenarios. To visualize the cyclical structure more clearly, we plot phase portraits of the delayed variables. Figures 5 and 6 show the relationships between $p(t)$ and $p(t-D)$, and between $b(t)$ and $b(t-D)$, respectively. The resulting closed curves confirm the presence of a stable limit cycle. These portraits

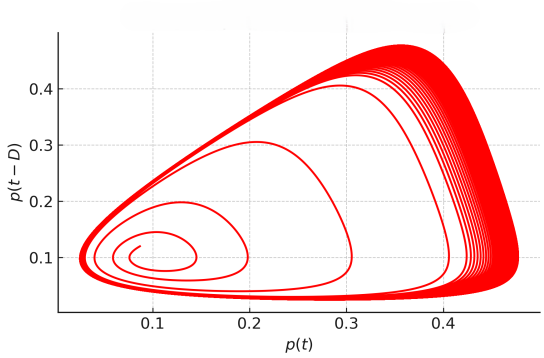

Fig. 5 Phase plot: $p(t)$ vs $p(t-D)$ for $D=4$

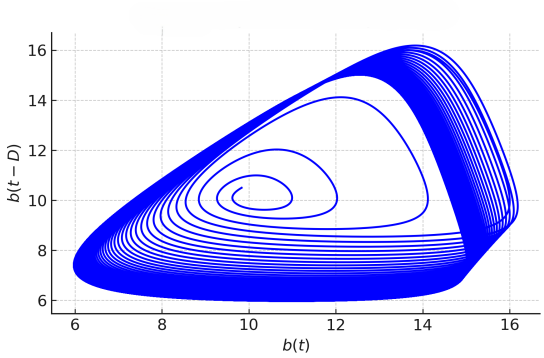

Fig. 6 Phase plot: $b(t)$ vs $b(t-D)$ for $D=4$

highlight the critical role of communication delays in shaping the nonlinear dynamics of congestion control systems.

Remark 5.1. The previous simulations validate the analytical predictions derived from Hopf bifurcation theory and underscore the destabilizing role of communication delays in REM-based feedback systems. From a control design standpoint, the results stress the importance of delay-aware tuning strategies. Economically, they demonstrate that even decentralized algorithms with strong theoretical guarantees can experience endogenous instability under realistic network delays, which may necessitate delay compensation, memory smoothing, or adaptive gain control to ensure global performance.

5.1 Comparison with the Discrete Delay Model

The REM model by [1] uses a constant, discrete delay to analyze Hopf bifurcation, assuming uniform round-trip times, an unrealistic simplification for real networks. We extend this by introducing gamma-distributed delays to better capture the stochastic nature of queuing, routing, and protocol variability. Unlike the discrete case, where stability breaks sharply at a critical delay D_0, the distributed-delay model, especially under strong memory ($m=2$), features a smoother transition across a delay interval $[T_1^*, T_2^*]$, improving robustness. Economically, distributed delays average feedback over time, dampening overreactions, reducing price volatility, and enabling fairer, more resilient congestion control, especially valuable in heterogeneous and delay-sensitive networks. The red curve, based on the discrete-delay model of [1], shows a sharp jump in oscillation amplitude immediately after the threshold $D_0 \approx 3.12$. This abrupt change suggests fragility to delay variation and a narrow operating window for stability. In contrast, the blue curve representing our distributed-delay formulation exhibits a gradual rise in oscillation amplitude across a bounded delay interval. This smoother transition suggests that distributed memory buffers the system against delay shocks. As a result, the network remains stable under a wider range of round-trip times, even as congestion builds. These visual and analytical distinctions highlight the superior dynamical and economic performance of distributed-delay congestion control models. They provide a compelling case for transitioning from deterministic delay modeling to more realistic and robust delay-aware designs.

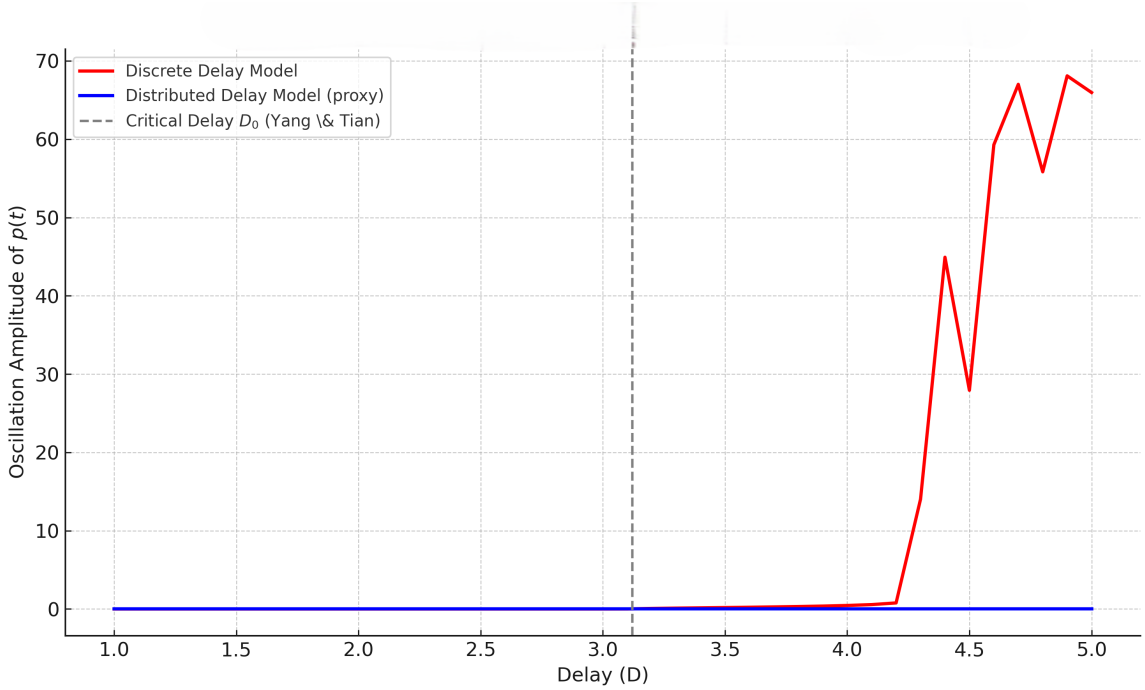

Fig. 7 Comparison of bifurcation behavior in discrete-delay (red) and distributed-delay (blue) REM models.

6 Conclusions and future research

This paper presented a bifurcation analysis of a REM-based congestion control system incorporating gamma-distributed feedback delays. By extending the classical discrete-delay REM framework of [1], we modeled memory effects using gamma kernels and derived equivalent ODE systems via the linear chain trick. Our analysis revealed that delay-induced instability manifests through Hopf bifurcations, with critical thresholds depending on the delay distribution's shape and memory parameter. For weak memory ($m = 1$), a single critical delay governs the transition from stability to periodic oscillations. In contrast, strong memory ($m = 2$) produces a bounded delay interval over which bifurcation can occur. These findings highlight the smoother and more robust behavior of distributed-delay models compared to their discrete-delay counterparts. Numerical simulations validated the theoretical predictions and confirmed that distributed delays buffer the system against sharp instability transitions. Economically, this translates into more stable congestion pricing and fairer bandwidth allocation under realistic network conditions. Future research may explore several extensions. First, incorporating time-varying or state-dependent delay distributions could offer further realism in modeling delay heterogeneity. Second, applying control-theoretic strategies such as adaptive gain tuning or delay compensation could improve robustness in dynamic environments. Finally, extending the analysis to networked systems with multiple coupled REM links would provide a more comprehensive view of distributed congestion control in large-scale infrastructures.

References

[1] H.Y. Yang, Y.P. Tian. Hopf bifurcation in REM algorithm with communication delay. Chaos, Solitons & Fractals, 25:1093–1105, 2005.

[2] B.D. Hassard, N.D. Kazarinoff, Y.H. Wan. Theory and Applications of Hopf Bifurcation. Cambridge University Press, 1981.

[3] S.H. Low, D.E. Lapsley. Optimization flow control—I: Basic algorithm and convergence. IEEE/ACM Transactions on Networking, 7:861–874, 1999.

[4] S. Athuraliya, S.H. Low, Q. Yin. REM: Active queue management. IEEE Network, 15:48–53, 2001.

[5] Q. Yin, S.H. Low. Convergence of REM flow control at a single link. IEEE Communications Letters, 5:119–121, 2001.

[6] Q. Yin, S.H. Low. On stability of REM algorithm with uniform delay. In: Proc. IEEE GLOBECOM, pp. 2649–2653, 2002.

[7] F. Paganini. A global stability result in network flow control. Systems & Control Letters, 46:165–172, 2002.

[8] C. Li, G. Chen, X. Liao, J. Yu. Hopf bifurcation in an Internet congestion control model. Chaos, Solitons & Fractals, 19:853–862, 2004.

[9] Y.P. Tian, H.Y. Yang. Stability of the Internet congestion control with diverse delays. Automatica, 40:1533–1541, 2004.

[10] Y. Cao. Bifurcations in an Internet congestion control system with distributed delay. Applied Mathematics and Computation, 347:54–63, 2019.

[11] L. Wang, W. Qin, Y.Y. Zhao. Dynamic properties of dual-delay network congestion control system based on hybrid control. Neural Processing Letters, 55:9295–9314, 2023.

[12] M.M. Bahnasy, H. Elbiaze, B. Boughzala. HetFlow: A distributed delay-based congestion control for data centers to achieve ultra-low queuing delay. In: IEEE International Conference on Communications (ICC), pp. 1–7, 2017.

[13] Y. Geng, H. Zhang, X. Shi, J. Wang, X. Yin, D. He, Y. Li. Delay-based congestion control for cross-datacenter networks. In: IEEE/ACM International Symposium on Quality of Service (IWQoS), pp. 1–4, 2023.

[14] Annu, R. Pachamuthu. Enhancing Sidelink 5G V2V Communication: A distributed probabilistic congestion control for dynamic resource allocation. In: IEEE International Conference on Advanced Networks and Telecommunications Systems (ANTS), pp. 1–6, 2023.

[15] S. Mynbayeva, A.T. Assanova, R.E. Uteshova. A solution to a linear boundary value problem for an impulsive integro-differential equation. Differential Equations and Dynamical Systems, 31:1–21, 2023.

[16] S. Moi, S. Biswas, S.P. Sarkar. Finite-difference method for fuzzy singular integro-differential equation deriving from fuzzy nonlinear differential equation. Granular Computing, 8:503–524, 2022.

[17] A. Singh, N. Srivastava, S. Singh, V. Singh. Computational technique for multi-dimensional non-linear weakly singular fractional integro-differential equation. Chinese Journal of Physics, 80:305–333, 2022.

[18] K. Muthuselvan, B. Sundaravadivoo, S. Alsaeed, K.S. Nisar. New interpretation of topological degree method of Hilfer fractional neutral functional integro-differential equation with nonlocal condition. AIMS Mathematics, 8:17154–17170, 2023.

[19] V. Vlasov, N.A. Rautian. Spectral properties of the generator of a semigroup generated by the Volterra integro-differential equation. Differential Equations, 59:283–288, 2023.